THE JOURNAL OF BIOLOGICAL CHEMISTRY VOL. 287, NO. 45, pp. 38305–38315, November 2, 2012

Inactivation of MARK4, an AMP-activated Protein Kinase (AMPK)-related Kinase, Leads to Insulin Hypersensitivity and Resistance to Diet-induced Obesity*

Received for publication, June 6, 2012, and in revised form, September 13, 2012 Published, JBC Papers in Press, September 19, 2012, DOI 10.1074/jbc.M112.388934

Chao Sun[‡§1], **Liang Tian**[‡§1], **Jia Nie**[§¶], **Hai Zhang**[§], **Xiao Han**[¶], **and Yuguang Shi**[§2]

From the [‡]*College of Animal Science and Technology, Northwest A&F University, Yangling 712100, China, the* [§]*Department of Cellular and Molecular Physiology, Pennsylvania State University College of Medicine, Hershey, Pennsylvania 17033, and the* [¶]*Key Laboratory of Human Functional Genomics of Jiangsu Province, Nanjing Medical University, Nanjing 210029, China*

Background: MARK4 is a member of the AMPK-related kinase family whose biological function remains elusive.
Results: Using mice with targeted deletion of *mark4*, we identified a key role of the kinase in regulating glucose and energy homeostasis.
Conclusion: MARK4 is required for energy homeostasis by regulating satiety and the metabolic rate in rodents.
Significance: These data provide a key insight for targeting MARK4 for the treatment of obesity.

MARK4, also known as Par-1d/MarkL1, is a member of the AMP-activated protein kinase (AMPK)-related family of kinases, which are implicated in the regulation of dynamic biological functions, including glucose and energy homeostasis. However, the physiological function of MARK4 in mammals remains elusive. Here, we investigated a role for MARK4 in regulating energy homeostasis by generating mice with targeted inactivation of the *mark4* gene. We show that MARK4 deficiency in mice caused hyperphagia, hyperactivity, and hypermetabolism, leading to protection from diet-induced obesity and its related metabolic complications through up-regulation of brown fat activity. Consequently, MARK4 deficiency mitigated insulin resistance associated with diet-induced obesity by dramatically enhancing insulin-stimulated AKT phosphorylation in major metabolic tissues. Ablation of MARK4 also significantly improved glucose homeostasis by up-regulating the activity and expression of AMPK kinase in key metabolic tissues. Taken together, these data identify a key role of MARK4 in energy metabolism, implicating the kinase as a novel drug target for the treatment of obesity and type 2 diabetes.

Microtubule affinity regulatory kinases (MARKs),[3] which represent the mammalian homologs of nematode *par-1*, were originally identified by their ability to phosphorylate microtubule-associated proteins, thus regulating microtubule stability in cultured cells (1). Par-1 is an evolutionarily conserved protein kinase required for polarity in worms, flies, frogs, and mammals (2–4). The mammalian Par-1 family consists of four members (Par-1c/Mark1, Par-1b/Mark2/Emk, Par-1a/Mark3/C-TAK1, and Par-1d/Mark4/KarkL1), each encoded by a distinct gene that is selectively expressed in multiple tissues (5). The physiological functions of the MARK2 and MARK3 kinases have recently been studied using targeted gene knockout approaches in mice (5, 6). Two independently derived mouse lines null for MARK2 have implicated this protein kinase in diverse physiological processes, including fertility (7), immune system homeostasis (8), learning and memory (9), and glucose homeostasis and energy metabolism (6). In addition to MARK2, most information regarding the cell biological functions of the Par-1 kinase comes from studies of MARK3. Specifically, MARK3 has been implicated in pancreatic tumors (10) and hepatocarcinogenesis (11), as well as in colorectal tumors (12). Loss of MARK3 also leads to reduced adiposity, resistance to hepatic steatosis, and defective gluconeogenesis. However, the functional roles of MARK1 and MARK4 remain elusive.

MARK kinases are members of the AMP-activated protein kinase (AMPK)-related family of kinases. AMPK is a key regulator of energy homeostasis and is activated in response to an increase in the AMP/ATP ratio under low-nutrient conditions (13–15). Other members of the AMPK family are implicated in regulating energy homeostasis, which is underscored by the phenotype of mice with targeted disruption of LKB1, a master upstream kinase of MARK4 and 11 other members of the AMPK-related kinase family (16–24). Targeted disruption of LKB1 in adult pancreatic β-cells significantly increases β-cell mass and insulin secretion in LKB1-null mice, whereas selective LKB1 ablation in skeletal muscle improves insulin sensitivity and glucose utilization (16, 17, 21). The phenotype of LKB1 knock-out mice is certainly compromised by diverse biological roles of the AMPK-related family of kinases. For example, AMPK has been shown to improve insulin sensitivity and glycemic control, and AMPK activators have been developed to reverse the metabolic abnormalities associated with type 2 diabetes mellitus (13, 15). In contrast, targeted disruption of either MARK2 or MARK3, two AMPK-related kinases, leads to hypoinsulinemia and resistance to diet-induced obesity and its

* This work was supported, in whole or in part, by National Institutes of Health Grant DK076685 (to Y. S.). This work was also supported by a scholarship from the China Scholarship Council (to L. T.).
[1] Both authors contributed equally to this work.
[2] To whom correspondence should be addressed: Dept. of Cellular and Molecular Physiology, Pennsylvania State University College of Medicine, 500 University Dr., H166, Hershey, PA 17033. Tel.: 717-531-0003; Fax: 717-531-7667; E-mail: yus11@psu.edu.
[3] The abbreviations used are: MARK, microtubule affinity regulatory kinase; AMPK, AMP-activated protein kinase; RER, respiratory exchange ratio; CLAMS, comprehensive laboratory animal monitoring system.

related insulin resistance (6, 25). Finally, in contrast to the well characterized roles of AMPK in metabolism (15), little is known about the regulatory function of other members of the AMPK kinase family, including MARK4, in glucose and energy homeostasis.

The MARK kinase family has been shown to phosphorylate tau, a microtubule-associated protein found in a hyperphosphorylated state in neurons of patients with Alzheimer disease, thus implying a potential role of MARK4 in Alzheimer disease (26, 27). This hypothesis is supported by genetic linkage analysis, which links polymorphism of the *MARK4* locus with the onset of Alzheimer disease (28). In this study, to determine the essential biological functions of MARK4, we generated mice with a disrupted *mark4* gene. We demonstrate that MARK4-null mice displayed a number of striking changes in metabolic parameters, including reduced adiposity, insulin hypersensitivity, and resistance to high-fat diet-induced weight gain. These findings elucidate a role for MARK4 in the regulation of both glucose homeostasis and energy balance, implicating MARK4 as a novel drug target for metabolic diseases.

EXPERIMENTAL PROCEDURES

Reagents—The antibodies used in this study included polyclonal antibodies to MARK4, AKT, phospho-AKT (Ser-473), AMPKα, phospho-AMPKα (Thr-172), and phospho-stress-activated protein kinase/JNK (Thr-183/Tyr-185), all of which were purchased from Cell Signaling Technology (Danvers, MA). Polyclonal antibodies to JNK1 were from Santa Cruz Biotechnology (Santa Cruz, CA). Horseradish peroxidase-conjugated donkey anti-rabbit IgG antibodies were purchased from GE Healthcare.

Animal Care—All animal experiments were approved by the Institutional Animal Care and Use Committee of the Pennsylvania State University College of Medicine in compliance with approved institutional animal care and use protocols according to National Institutes of Health guidelines (publication 86-23, 1985). Animals were maintained in an environmentally controlled facility with a diurnal light cycle and free access to water and either standard rodent chow (2018 Teklad global 18% protein rodent diet, Harlan Laboratories, Inc., Madison, WI) or a high-fat diet (catalog no. D12492, Research Diets, Inc., New Brunswick, NJ).

Oral Glucose and Insulin Tolerance Tests—These tests were performed in overnight food-deprived mice ($n = 10$). Glucose was delivered by oral gavage at 2.5 g/kg of body weight after initial measurement of fasting blood glucose. Insulin was delivered by intraperitoneal injection (0.75 units/kg of body weight; Novolin, Novo Nordisk). Blood glucose was determined 0, 30, 60, 90, and 120 min after the glucose or insulin load using a One Touch Ultra 2 glucometer (LifeScan, Inc., Milpitas, CA). All studies were carried out in MARK4$^{-/-}$ mice after two generations of backcrossing with an C57BL/6 inbred strain.

Generation of MARK4 Knock-out Mice—A mouse embryonic stem cell clone carrying a retroviral disruption of exon 8 of the *mark4* gene was generated by the International Gene Trap Consortium. The use of the Engrailed-2 splicing acceptor site in the retroviral vector generated a fusion message between exon 8 of the *mark4* gene and β-galactosidase-neomycin resistance gene fusion (β-*geo*) cDNA, truncating *mark4* after the first 198 amino acid residues, right in the middle of the kinase domain. The embryonic stem cells were microinjected by the University of California, Davis, mouse service. Heterozygous MARK4 knock-out founder mice were identified by genomic PCR using primer pairs for the β-*geo* cassette and primer pairs for the disrupted exon (see Fig. 1*A*) and confirmed by Southern blot analysis using a DNA probe isolated from the genomic intron sequence 5′ to exon 8 of the mouse *mark4* locus. Homozygous MARK4 knock-out mice were generated from an intercross of heterozygous MARK4 knock-out mice. Southern blot analysis was carried out using genomic DNA predigested with SacI enzyme.

Body Composition, Energy Expenditure, Activity, and Food Intake—Body fat and lean body mass were measured using an LF90 TD-NMR analyzer (Bruker Optics). Measurements of food/water intake, energy expenditure, respiratory exchange ratio (RER), and physical activity were performed using metabolic cages equipped with a comprehensive laboratory animal monitoring system (CLAMS; TSE Systems, Bad Homburg, Germany). Constant airflow (0.4 liters/min) was drawn through the chamber and monitored by a mass-sensitive flow meter. The concentrations of oxygen and carbon dioxide were monitored at the inlet and outlet of the sealed chambers to calculate oxygen consumption and respiratory quotient. Each chamber was measured for 1 min at 15-min intervals. Physical activity was measured using infrared technology (OPT-M3, Columbus Instruments) as the count of three-dimensional beam breaking (*X* total, *X* ambulatory, and *Z*).

Serum Factor Quantification—Serum levels of insulin, triglycerides, and cholesterol were determined by Ani Lytics Inc. (Gaithersburg, MD; $n = 8–10$ animals per genotype and sex).

Western Blot Analysis—For analysis of insulin signaling from tissue samples, MARK4$^{-/-}$ mice and controls were fasted overnight, followed by intraperitoneal injection of insulin (1 unit/kg of body weight) or PBS, and then killed 10 min after the injection. Tissues were rapidly dissected and frozen in liquid nitrogen. The tissue samples were then pulverized in liquid nitrogen and homogenized in radioimmune precipitation assay buffer (20 mM Hepes, 2 mM EGTA, 50 mM NaF, 100 mM KCl, 0.2 mM EDTA, 50 mM β-glycerophosphate, 1.5 mM Na_3VO_4, 10 mM Na_4VO_7, 1 mM benzamidine, 100 μl of phosphatase inhibitor mixture, 1% Triton X-100, and 1.0 mM PMSF) with a Polytron homogenizer. After a 30-min incubation on ice, the samples were centrifuged at 10,000 $\times$ *g* for 10 min at 4 °C. The protein concentration was determined by Pierce BCA protein assay (Thermo Scientific). Equal amounts of protein (30 μg) were subjected to SDS-PAGE, transferred to PVDF membrane (Bio-Rad), blocked in Tris-buffered saline with 5% milk, immunoblotted with primary antibodies (1:1000) overnight at 4 °C followed by secondary antibodies (1:2500) for 1 h at room temperature, and developed using the ECL Plus system (GE Healthcare).

Statistical Analysis—Statistical comparisons were done using the two-tailed unpaired *t* test to determine differences between MARK4$^{-/-}$ and WT mice. Analysis of covariance was also used to assess differences between MARK4$^{-/-}$ and WT mice in metabolic parameters relative to total body weight and

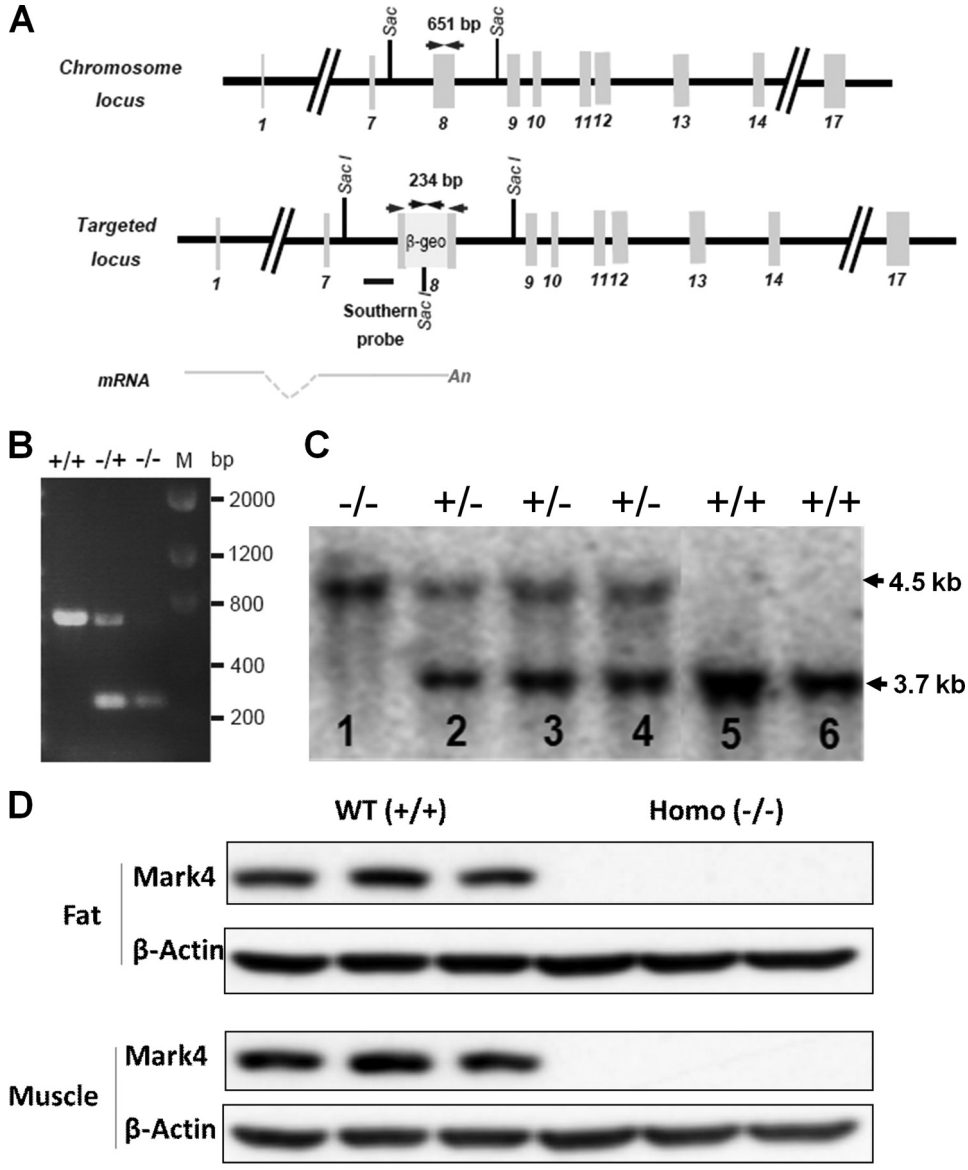

FIGURE 1. **Generation of mice with targeted disruption of the *mark4* gene.** *A*, gene trap insertion at the *mark4* locus. Retrovirus-mediated insertion of the *β-geo* gene caused premature termination of the *mark4* gene after the first 198 amino acids, right in the middle of the kinase domain. *An*, polyadenylation signal. *B*, PCR analysis of genotypes, resulting in a 651-bp product for the *mark4* allele and a 234-bp product for the *β-geo* insertion. *M*, molecular mass markers. *C*, Southern blot analysis of the *mark4* locus using genomic DNA predigested with the SacI restriction enzyme, which resulted in detection of a 3.7-kb DNA band for the WT allele and a 4.5-kb DNA band for the null allele. *D*, Western blot analysis of MARK4 protein expression in isolated fat and skeletal muscle tissues of homozygous MARK4 knock-out (−/−), heterozygous MARK4 knock-out mice (+/−), and WT control mice (+/+) using anti-MARK4 antibodies and *β*-actin as an internal control for protein loading (n = three mice per genotype per tissue).

lean body mass. Values are presented as means ± S.E.; $p < 0.05$ was considered significantly different.

RESULTS

Generation of Mice with Targeted Disruption of the mark4 Gene—To investigate a role for MARK4 in glucose and energy homeostasis, we generated mice with targeted disruption of the *mark4* gene by retrovirus-mediated insertion of the *β-geo* cassette in exon 8, leading to premature termination of the coding region of the *mark4* gene (Fig. 1*A*). Genotypes of homozygous ($MARK4^{-/-}$) and heterozygous ($MARK4^{+/-}$) MARK4 mice and the WT controls ($MARK4^{+/+}$) were analyzed by PCR analysis (Fig. 1*B*). Southern blot analysis demonstrated the predicted sizes of the mutant and WT *mark4* alleles (Fig. 1*C*). Deletion of *mark4* resulted in a total absence of MARK4 protein, as confirmed by Western blot analysis using anti-MARK4 antibodies and tissue lysate from the fat and skeletal muscle of $MARK4^{-/-}$ mice (Fig. 1*D*).

MARK4 $^{-/-}$ Mice Are Protected from Diet-induced Obesity and Insulin Resistance—The $MARK4^{-/-}$ mice were born at the predicted Mendelian ratios without any obvious phenotypic abnormality when fed standard mouse chow for 8 weeks. The $MARK4^{-/-}$ mice were backcrossed with a C57BL/6 inbred strain for two generations, followed by metabolic studies. Key metabolic studies were also repeated in mice with a pure C57BL/6 genetic background, which was achieved by seven consecutive generations of backcrossing with the C57BL/6 strain. Female $MARK4^{-/-}$ mice with a mixed genetic back-

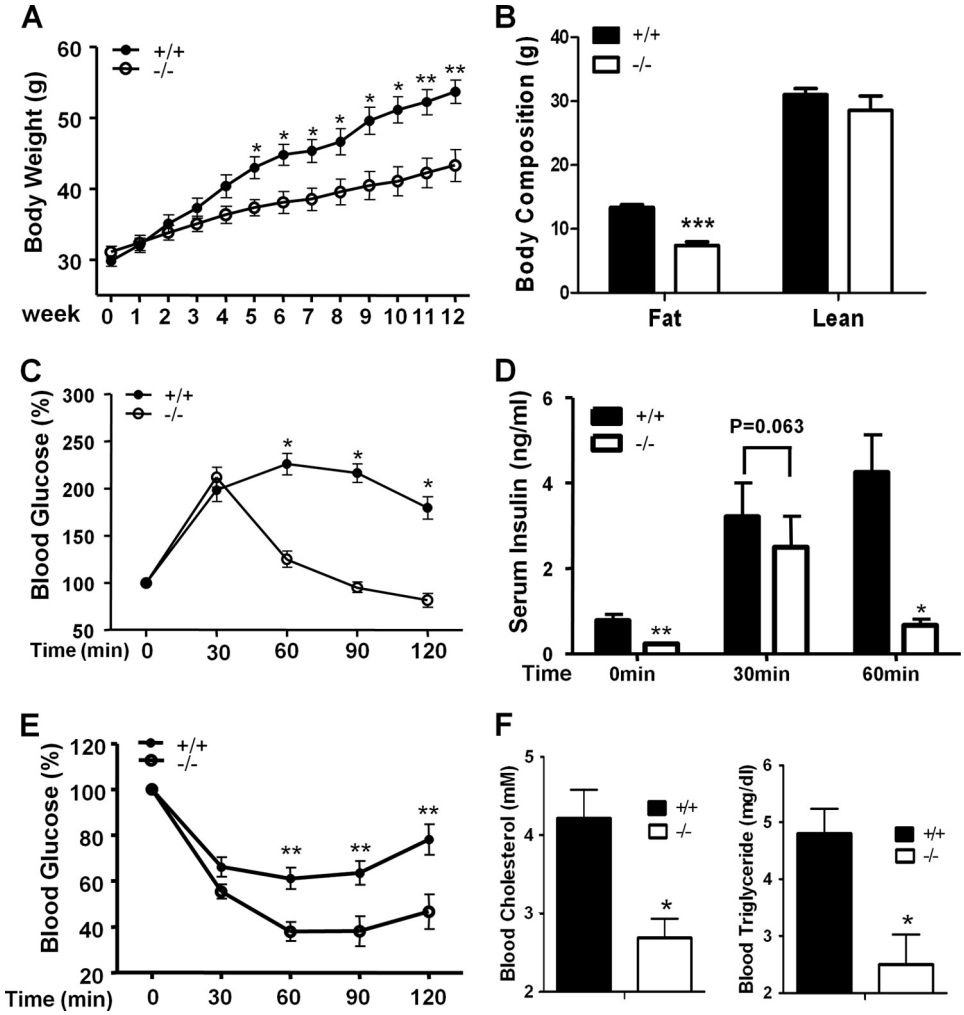

FIGURE 2. **MARK4$^{-/-}$ mice are protected from the onset of diet-induced obesity and its related insulin resistance.** Male MARK4$^{-/-}$ mice (−/−) and WT control mice (+/+), 8 weeks old, were fed diet with 60% fat for 12 consecutive weeks, followed by analysis for weight gain (*A*); body composition by magnetic resonance imaging (*B*); blood glucose levels during a oral glucose tolerance test (*C*); serum insulin levels at 0, 30, and 60 min during a glucose tolerance test (*D*); blood glucose levels during a insulin tolerance test (*E*); and cholesterol and triglyceride blood levels (*F*) ($n = 8$–10). *, $p < 0.05$; **, $p < 0.01$ compared with WT controls.

ground or a pure C57BL/6 background were indistinguishable from WT controls with regard to body weight when fed regular chow at 8 weeks of age. After being fed a high-fat diet containing 60% calories from animal fat for 12 consecutive weeks, the weight gain in MARK4$^{-/-}$ mice was significantly lower in male mice (Fig. 2*A*), but not in female mice, compared with the WT control mice. The difference was due entirely to decreased fat mass in MARK4$^{-/-}$ mice as measured by ^{1}H magnetic resonance imaging (Fig. 2*B*). The total body fat content was 15% higher in WT mice than in MARK4$^{-/-}$ mice, suggesting a role for MARK4 in diet-induced obesity. The results were further confirmed using MARK4$^{-/-}$ mice with a pure C57BL/6 background (data not shown).

We next analyzed changes in glucose homeostasis and insulin sensitivity in the MARK4$^{-/-}$ mice relative to the WT sibling controls. After an overnight fast, blood glucose levels were indistinguishable between the MARK4$^{-/-}$ mice and the WT controls. However, blood glucose levels in the MARK4$^{-/-}$ mice were significantly lower than those in the WT control mice as determined by a oral glucose tolerance test (Fig. 2*C*). Despite an improvement in glucose excursion, the serum insulin levels in the MARK4$^{-/-}$ mice were significantly lower those in the WT control mice after overnight fasting and at 60 min after glucose challenge (Fig. 2*D*), suggesting an enhancement of insulin sensitivity. Indeed, in comparison with WT control mice, the MARK4$^{-/-}$ mice were more sensitive to hypoglycemia induced by insulin injection as determined by an insulin tolerance test (Fig. 2*E*). Consistent with reduced adiposity and improved glucose tolerance, MARK4-null mice also exhibited significantly lower levels of blood triglycerides and cholesterol compared with WT control littermates (Fig. 2*F*). Because both genders of the heterozygous MARK4 knock-out mice and the female MARK4$^{-/-}$ mice were not significantly different from the WT controls with regard to weight gain and insulin/glucose tolerance, subsequent studies were carried out only in male MARK4$^{-/-}$ mice and control mice.

Hyperphagia, Hyperactivity, and Increased Energy Expenditure in MARK4$^{-/-}$ Mice—To determine the mechanisms by which MARK4 regulates the onset of diet-induced obesity and insulin sensitivity, we next analyzed changes in food and water

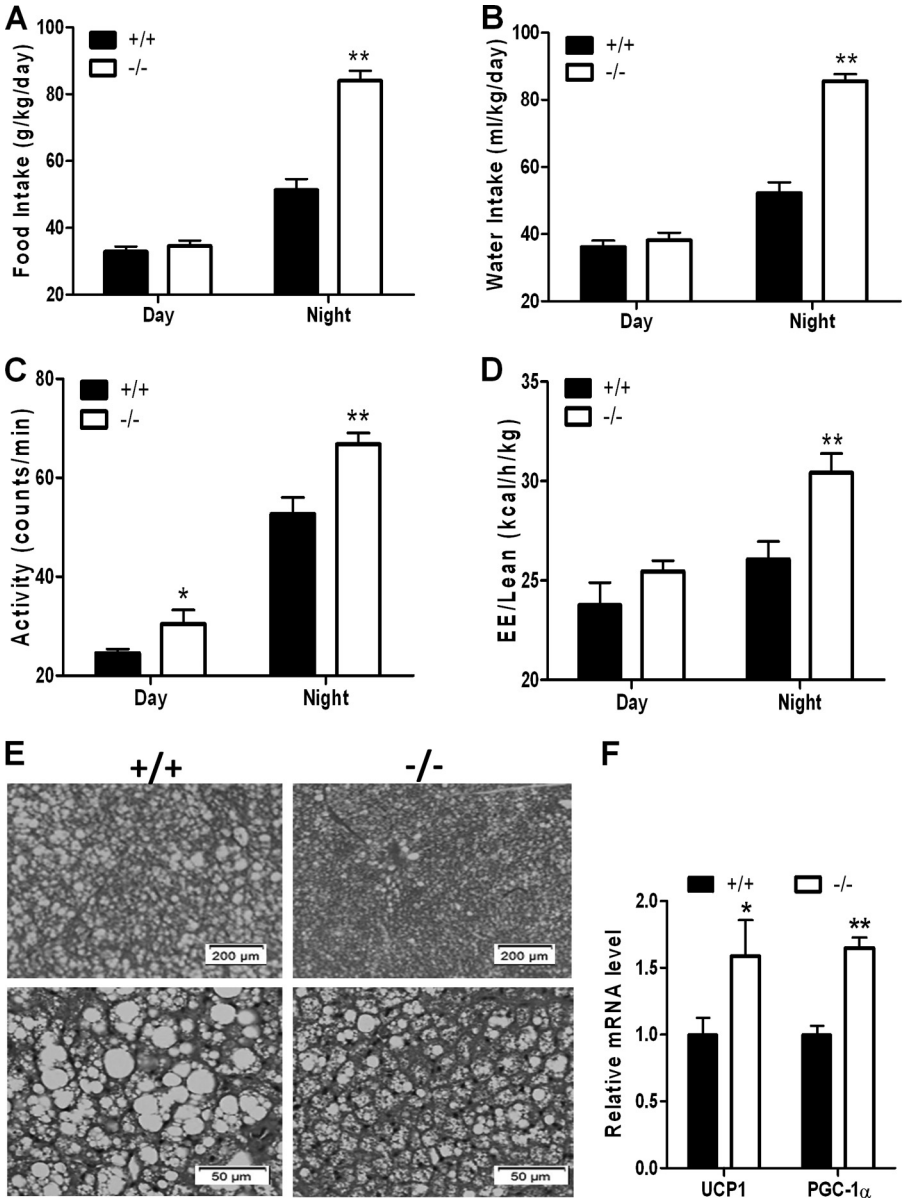

FIGURE 3. **Hyperphagia, hyperactivity, and hypermetabolism in MARK4$^{-/-}$ mice.** Male MARK4$^{-/-}$ mice (−/−) and WT control mice (+/+), 8 weeks old, were fed a diet with 60% fat for 12 consecutive weeks, followed by analysis for diurnal food intake (*A*), water intake (*B*), physical activity (*C*), and energy expenditure (*EE*) normalized to lean body mass (*D*) over 24 h in a metabolic cage equipped with CLAMS. *E*, H&E staining of brown adipose tissue. *F*, analysis of mRNA expression of UCP1 and PGC-1α in brown adipose tissue ($n = 8$–10). *, $p < 0.05$; **, $p < 0.01$ compared with WT controls.

intake, physical activity, and energy expenditure in the male MARK4$^{-/-}$ mice relative to the WT control mice over 72 h by housing the mice in metabolic cages equipped with CLAMS. As shown in Fig. 3 (*A* and *B*), the lean phenotype of the MARK4$^{-/-}$ mice was not caused by reduced food intake because they consumed twice as much food and water during the night compared with the WT control mice. In contrast, the food and water intake was not different between the MARK4$^{-/-}$ and WT control mice during the day. The MARK4$^{-/-}$ mice were also hyperactive, as evidenced by enhanced physical activity relative to the WT control mice (Fig. 3*C*). Consequently, the energy expenditure rate was significantly higher in MARK4$^{-/-}$ mice (Fig. 3*D*) when normalized to lean body mass. Consistent with the increased energy expenditure in MARK4$^{-/-}$ mice, the brown adipose tissue from MARK4$^{-/-}$ mice exhibited significantly smaller lipid droplets (Fig. 3*E*). Furthermore, the mRNA expression of both UCP1 and PGC-1α was significantly up-regulated in brown adipose tissue (Fig. 3*F*), suggesting increased brown adipose activity in the MARK4$^{-/-}$ mice.

MARK4 Deficiency Increases Oxygen Consumption, CO_2 Production, and RER in MARK4$^{-/-}$ Mice—Hyperphagia but with reduced adiposity in MARK4$^{-/-}$ mice prompted us to investigate a role for MARK4 in regulating the metabolic rate by CLAMS. We measured oxygen consumption (VO_2), CO_2 production, and RER over 24 h in the metabolic cage. Consistent with the increased energy expenditure, MARK4$^{-/-}$ mice consumed significantly higher levels of oxygen (Fig. 4*A*; quantified in Fig. 4*B*) and thus produced more CO_2 than the control mice (Fig. 4*C*; quantified in Fig. 4*D*) during a 24-h period. RER measures the VCO_2/VO_2 ratio, which reflects the ratio of carbohy-

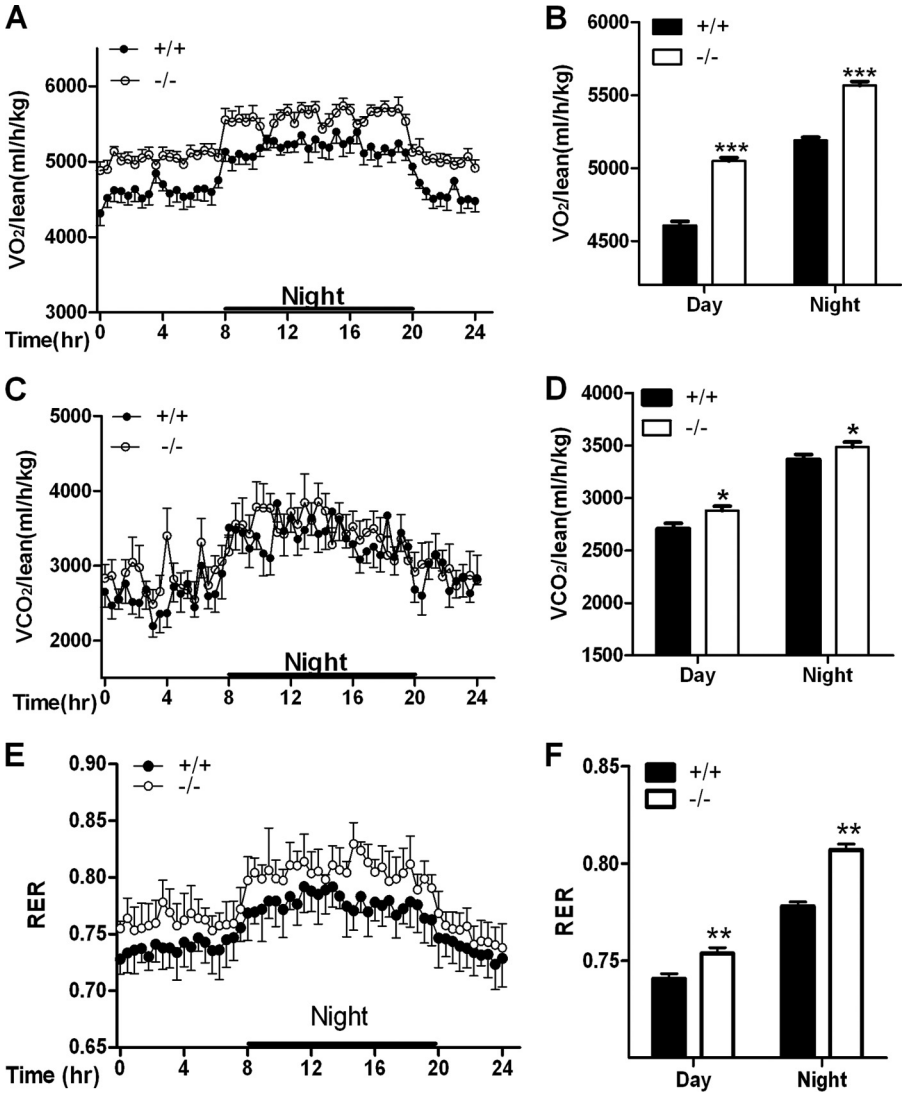

FIGURE 4. **Analysis of oxygen consumption, CO_2 production, and RER by CLAMS.** Male MARK4$^{-/-}$ mice (−/−) and WT control mice (+/+) from Fig. 3 were analyzed for changes in diurnal oxygen consumption normalized to lean body mass (*A* and *B*), CO_2 production normalized to lean body mass (*C* and *D*), and RER (*E* and *F*) over 24 h ($n = 8–10$). *, $p < 0.05$; **, $p < 0.01$ compared with WT controls.

drate and fat metabolism. A lower RER is an indication of greater fat metabolism, whereas a higher RER is an indication of greater carbohydrate metabolism. As a compensatory response to reduced adiposity, the RER was significantly higher in MARK4$^{-/-}$ mice relative to the WT control mice (Fig. 4*E*; quantified in Fig. 4*F*), suggesting that MARK4$^{-/-}$ mice consumed more carbohydrate as an energy source. The results were further confirmed in male MARK4$^{-/-}$ mice with a pure C57BL/6 background (data not shown).

Ablation of MARK4 Exacerbates Hyperphagia and Hypermetabolism after Starvation—Fasting RER and resting metabolic rate are good predictors of weight gain in humans (29). The hypermetabolism in MARK4$^{-/-}$ mice prompted us to investigate a role for MARK4 in regulating physical activity, oxygen consumption, RER, and energy expenditure during fasting and refeeding. As shown in Fig. 5*A* (quantified in Fig. 5*B*), the MARK4$^{-/-}$ mice consumed far more food during the refeeding period after 24 h of fasting. Although fasting reduced physical activity in both the MARK4$^{-/-}$ and control mice (Fig. 5*C*; quantified in Fig. 5*D*), the MARK4$^{-/-}$ mice remained more physically active during the fasting period. As a result, the MARK4$^{-/-}$ mice consumed significantly more oxygen (Fig. 5*E*; quantified in Fig. 5*F*) and released more CO_2 when normalized to lean body mass (Fig. 6*A*; quantified in Fig. 6*B*). Additionally, fasting significantly decreased the RER in both MARK4$^{-/-}$ and WT control mice, suggesting a switch to lipid oxidation as an energy source, yet the RER remained higher in MARK4$^{-/-}$ mice during fasting (Fig. 6*C*; quantified in Fig. 6*D*). In support of a role for MARK4 in regulating the basal metabolic rate, energy expenditure was significantly higher in MARK4$^{-/-}$ mice during the fasting period (Fig. 6*E*; quantified in Fig. 6*F*), which is consistent with exacerbated hyperphagia during the refeeding period (Fig. 5*A*).

MARK4 Deficiency Improves Insulin Signaling and Up-regulates AMPK Expression in MARK4$^{-/-}$ Mice—To gain further insight into the molecular mechanisms by which MARK4 regulates glucose homeostasis, we next analyzed the effect of MARK4 deficiency on insulin-stimulated AKT and AMPK sig-

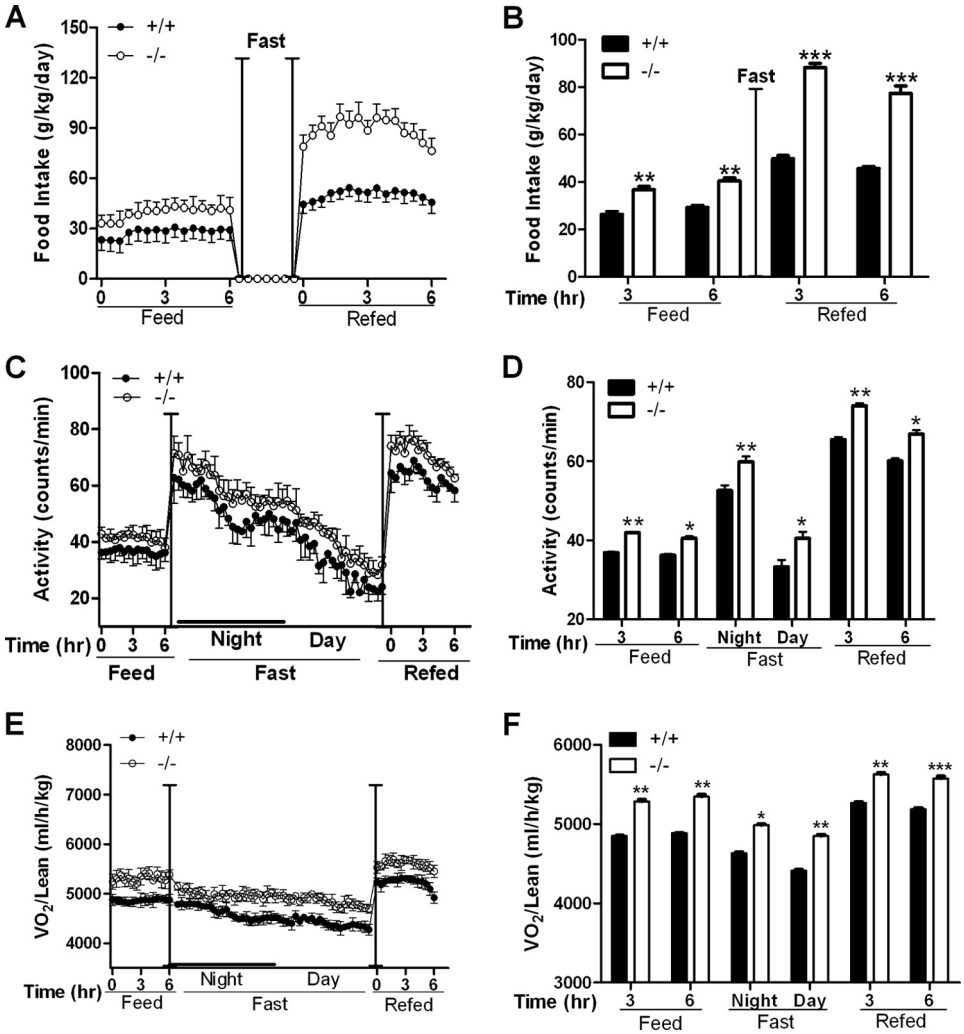

FIGURE 5. **MARK4 deficiency exacerbates hyperphagia after 24 h of fasting.** Male MARK4$^{-/-}$ mice (−/−) and WT control mice (+/+) from Fig. 3 were fasted for 24 h, followed by refeeding. MARK4-null mice exhibited remarkable hyperphagia during refeeding (*A* and *B*), hyperactivity (*C* and *D*), and increased oxygen consumption (*E* and *F*) during the fasting and refeeding period ($n = 8$–10 animals per genotype). *, $p < 0.05$; **, $p < 0.01$ compared with WT controls.

naling in major metabolic tissues, including white adipose tissue, skeletal muscle, liver, and heart. We focused on insulin-stimulated AKT-2 phosphorylation, which is impaired by insulin resistance associated with type 2 diabetes and obesity (30, 31). Consistent with insulin hypersensitivity in MARK4$^{-/-}$ mice, insulin-stimulated AKT phosphorylation was significantly enhanced in white adipose tissue, skeletal muscle, and liver (Fig. 7) relative to that in the WT controls. Impaired insulin-stimulated AKT phosphorylation in the heart is associated with cardiac dysfunction in type 2 diabetes (32). In further support of a role for MARK4 in regulating insulin signaling, MARK4 deficiency also significantly increased AKT phosphorylation in the hearts of MARK4$^{-/-}$ mice (Fig. 7*D*). Our data are supported by previous report that AKT expression and phosphorylation are significantly decreased in the aorta by the onset of type 2 diabetes (33). In contrast, there was no significant difference in JNK expression or phosphorylation between MARK4$^{-/-}$ and WT mice in these metabolic tissues (data not shown).

AMPK is an energy sensor that is activated in response to glucose deprivation, leading to catabolism to restore energy balance. AMPK in muscle is activated in response to exercise and treatment with metformin, an anti-diabetes drug, suggesting a key role for AMPK in the pathophysiology of type 2 diabetes (34). We next analyzed the consequence of MARK4 deficiency on AMPK activation and expression in the key metabolic tissues. Consistent with increased energy expenditure and reduced adiposity, MARK4 deficiency significantly stimulated phosphorylation of AMPK at Ser-172, a key activation site that is phosphorylated by LKB1 (35, 36), in skeletal muscle from the MARK4$^{-/-}$ mice (Fig. 7*B*). In further support of a role for MARK4 in AMPK regulation, ablation of MARK4 also significantly increased expression of the AMPK α-subunit in white adipose tissue (Fig. 7*A*).

DISCUSSION

The LKB1 kinase family, consisting of 12 members, is implicated in glucose and energy metabolism, as evidenced by the phenotype of mice with targeted disruption of LKB1 in various tissues (16–24). However, the phenotypes of LKB1-deficient mice are likely compromised by different biological functions among members of the AMPK-related kinase family. In con-

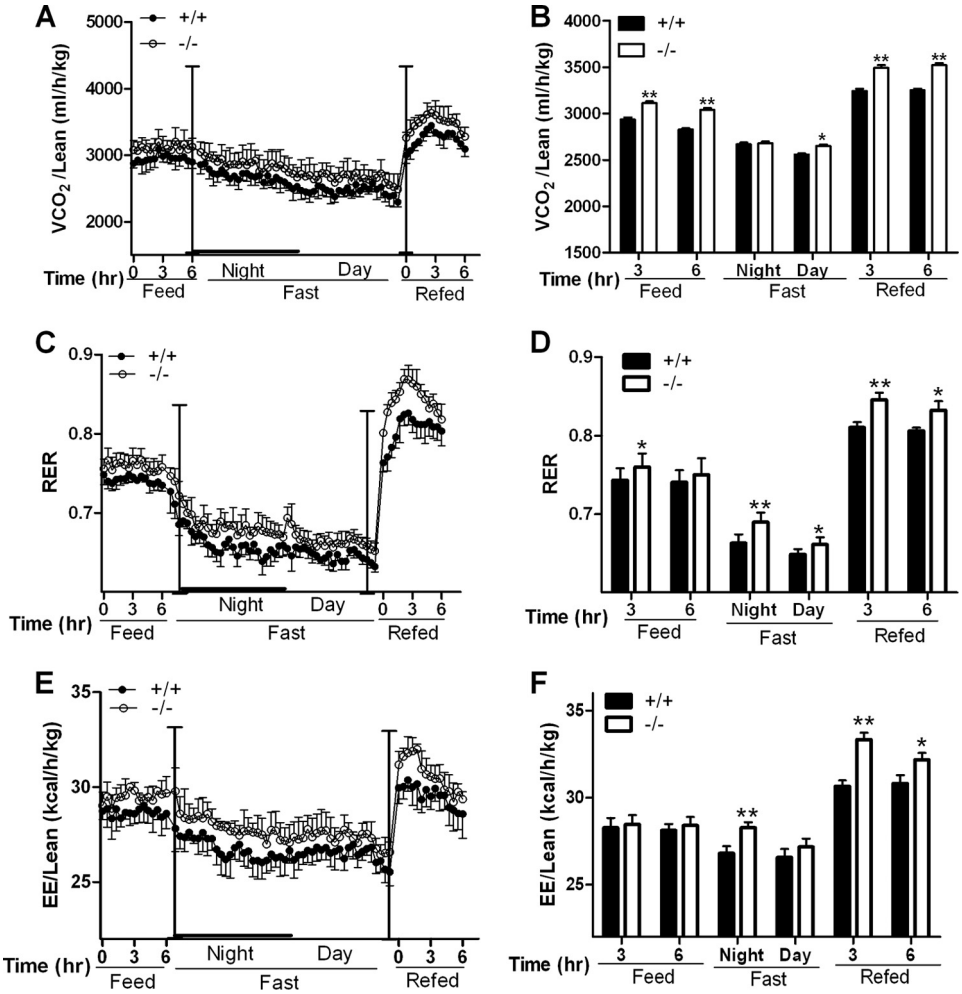

FIGURE 6. **Ablation of MARK4 increases basal energy expenditure.** Male MARK4$^{-/-}$ mice (−/−) and WT control mice (+/+) from Fig. 3 were fasted for 24 h, followed by refeeding. MARK4$^{-/-}$ mice exhibited elevated CO_2 production (*A* and *B*), RER (*C* and *D*), and energy expenditure (*EE*; *E* and *F*) during fasting, leading to increased basal energy metabolism ($n = 8–10$ animals per genotype). *, $p < 0.05$; **, $p < 0.01$ compared with WT controls.

trast to AMPK, little is known about the biological functions of other members in this family, including MARK4. In this study, we investigated a role for MARK4 in energy homeostasis in mice with targeted disruption of the *mark4* gene. We have shown that MARK4 deficiency in mice causes hyperphagia. Despite hyperphagia, the MARK4 knock-out mice were completely protected from diet-induced obesity due to increased physical activity and a higher basal metabolic rate. Consistent with the hypermetabolism, MARK4 deficiency significantly stimulated brown adipose activity, as evidenced by up-regulated mRNA expression of UCP1 and PGC-1α, key regulators of brown adipose activity. The reduced weight gain was caused entirely by decreased fat mass, resulting in a high content of lean whole body mass in MARK4$^{-/-}$ mice. Strikingly, MARK4 deficiency also dramatically improved insulin sensitivity, as evidenced by lower fasting serum insulin levels, improved insulin tolerance, and elevated insulin-stimulated AKT phosphorylation in all of the major metabolic tissues examined, including white adipose tissue, liver, skeletal muscle, and heart. The increased energy expenditure was independent of lean body mass and feeding, as the knock-out mice consumed more energy during 24 h of fasting and refeeding after normalization to lean body mass. Consequently, the MARK4 knock-out mice exhibited a significant improvement in glucose excursion and thus were protected from insulin resistance related to the onset of obesity. Together, these findings identify, for the first time, a key role for MARK4 in energy metabolism and insulin sensitivity.

In mammals, there are four isoforms of MARK kinases, MARK1–4, each encoded by a different gene with a distinct tissue distribution pattern. However, how these isoforms differ in their biological functions remains elusive. Recently, the physiological functions of the MARK2 and MARK3 kinases have been decoded in mice by using mice with targeted deletion of each gene (5, 6). Although both MARK2 and MARK3 knock-out mice share similar phenotypes with MARK4 knock-out mice, such as reduced adiposity, hypoinsulinemia, and hypermetabolism, there are fundamental phenotypic differences between MARK4-deficient mice and MARK2 and MARK3 knock-out mice in a number of notable features. First, MARK4 knock-out mice are fertile and are born with the predicted Mendelian ratio. The MARK4-null mice survive to adulthood and exhibit a normal growth rate when fed regular chow. In contrast, mice deficient in MARK2 or MARK3 exhibit hypofertility, lower birth weight, and growth retardation, suggesting an essential role for both MARK2 and MARK3 in development

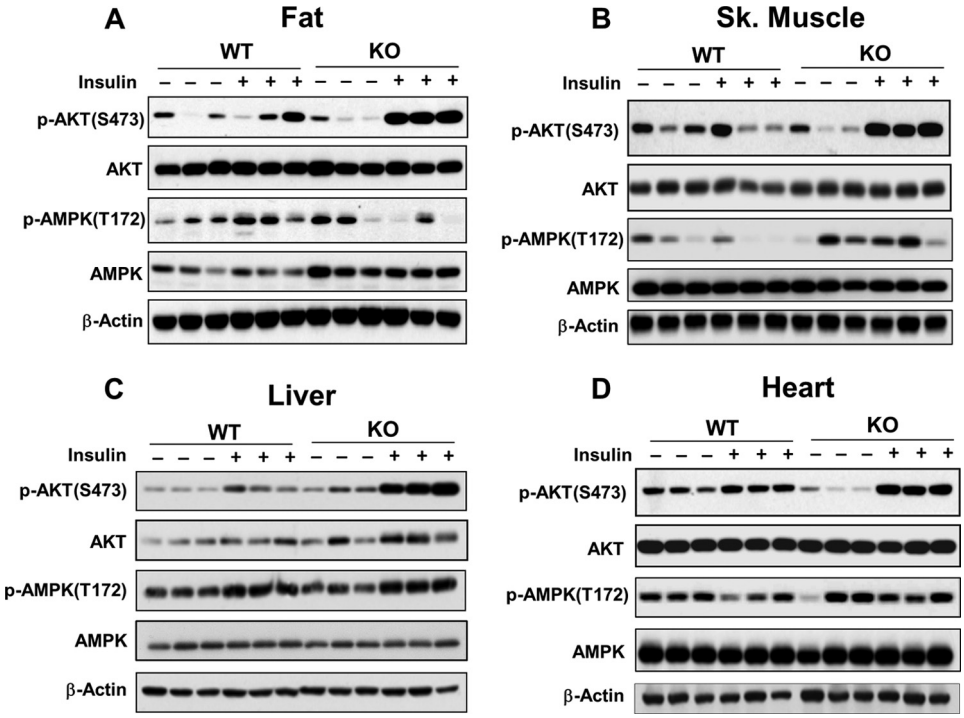

FIGURE 7. **MARK4 deficiency improves insulin signaling and stimulates AMPK expression.** Male MARK4$^{-/-}$ mice and WT control mice from Fig. 3 were fasted overnight and then injected intraperitoneally with insulin (1 unit/kg of body weight) or PBS, followed by Western blot analysis of insulin-stimulated AKT phosphorylation in white adipose tissue (*A*), skeletal muscle (*B*), liver (*C*), and heart (*D*). The same blots were also analyzed for phosphorylation of AMPK and the total protein level of each kinase using β-actin as an internal control for protein loading. MARK4 deficiency increased AKT phosphorylation in all tissues concurrently with increased AMPK phosphorylation in skeletal muscle and up-regulated AMPK expression in fat. *KO*, knock-out.

and growth. Additionally, MARK3 deficiency also causes other pathological side effects, including hepatic glycogen depletion, increased hepatocellular autophagy, and hypoketotic hypoglycemia. Consequently, mice that are deficient in both MARK2 and MARK3 are lethal. Furthermore, although MARK3-deficient mice are resistant to diet-induced obesity, MARK3 deficiency does not affect insulin sensitivity despite reduced adiposity. In contrast, MARK4 knock-out mice exhibit insulin hypersensitivity, as evidenced by hypoinsulinemia after overnight fasting and during a glucose tolerance test, severe hypoglycemia during a insulin tolerance test, and significantly enhanced insulin-stimulated AKT phosphorylation in major metabolic tissues.

In further support of a major role for MARK4 in energy metabolism, the study has identified MARK4 as a key regulator of AMPK expression and activity in multiple metabolic tissues. AMPK is the most intensively studied kinase among the 12 members of the LKB1 family of kinases due to its key role in regulating energy homeostasis and metabolic diseases (13, 15, 37). AMPK is expressed in key metabolically relevant organs, where it functions as a major cellular energy sensor. AMPK is activated in response to elevated intracellular levels of AMP associated with nutritional deficit to maintain energy homeostasis. In the liver, AMPK phosphorylates and inhibits sterol regulatory element-binding protein (SREBP) activity to attenuate hepatic steatosis and atherosclerosis in diet-induced insulin-resistant mice (38). Hepatic AMPK is also activated in response to treatment with metformin, a popular anti-diabetes drug, by suppressing the expression and activity of SREBP1, a key transcriptional activator required for lipid synthesis (36). In support of a role for MARK4 in AMPK expression, MARK4 deficiency significantly up-regulates AMPK expression in white adipose tissue. MARK4$^{-/-}$ mice also exhibit significantly lower levels of blood triglycerides and cholesterol, key indicators of obesity and its related metabolic complications. Furthermore, MARK4 deficiency also significantly stimulates AMPK phosphorylation in skeletal muscle. Our results are corroborated by previous reports that AMPK in skeletal muscle is activated in response to exercise, which improves insulin sensitivity (34), and that AMPK phosphorylation is significantly reduced in skeletal muscle in patients with type 2 diabetes and in a rodent model of obesity (39, 40). Taken together, our findings suggest that development of MARK4 inhibitors may provide a novel treatment for obesity and its related metabolic complications, including type 2 diabetes.

Acknowledgment—We are grateful to Dr. Leonard Jefferson for critically reading the manuscript.

REFERENCES

1. Drewes, G., Ebneth, A., Preuss, U., Mandelkow, E. M., and Mandelkow, E. (1997) MARK, a novel family of protein kinases that phosphorylate microtubule-associated proteins and trigger microtubule disruption. *Cell* **89,** 297–308
2. Saadat, I., Higashi, H., Obuse, C., Umeda, M., Murata-Kamiya, N., Saito, Y., Lu, H., Ohnishi, N., Azuma, T., Suzuki, A., Ohno, S., and Hatakeyama, M. (2007) *Helicobacter pylori* CagA targets PAR-1/MARK kinase to disrupt epithelial cell polarity. *Nature* **447,** 330–333
3. Goldstein, B., and Macara, I. G. (2007) The PAR proteins: fundamental players in animal cell polarization. *Dev. Cell* **13,** 609–622
4. Gomes, J. E., and Bowerman, B. (2002) *Caenorhabditis elegans par* genes.

Curr. Biol. **12,** R444
5. Hurov, J., and Piwnica-Worms, H. (2007) The Par-1/MARK family of protein kinases: from polarity to metabolism. *Cell Cycle* **6,** 1966–1969
6. Hurov, J. B., Huang, M., White, L. S., Lennerz, J., Choi, C. S., Cho, Y. R., Kim, H. J., Prior, J. L., Piwnica-Worms, D., Cantley, L. C., Kim, J. K., Shulman, G. I., and Piwnica-Worms, H. (2007) Loss of the Par-1b/MARK2 polarity kinase leads to increased metabolic rate, decreased adiposity, and insulin hypersensitivity *in vivo*. *Proc. Natl. Acad. Sci. U.S.A.* **104,** 5680–5685
7. Bessone, S., Vidal, F., Le Bouc, Y., Epelbaum, J., Bluet-Pajot, M. T., and Darmon, M. (1999) EMK protein kinase-null mice: dwarfism and hypofertility associated with alterations in the somatotrope and prolactin pathways. *Dev. Biol.* **214,** 87–101
8. Hurov, J. B., Stappenbeck, T. S., Zmasek, C. M., White, L. S., Ranganath, S. H., Russell, J. H., Chan, A. C., Murphy, K. M., and Piwnica-Worms, H. (2001) Immune system dysfunction and autoimmune disease in mice lacking Emk (Par-1) protein kinase. *Mol. Cell. Biol.* **21,** 3206–3219
9. Segu, L., Pascaud, A., Costet, P., Darmon, M., and Buhot, M. C. (2008) Impairment of spatial learning and memory in ELKL motif kinase 1 (EMK1/MARK2) knock-out mice. *Neurobiol. Aging* **29,** 231–240
10. Parsa, I. (1988) Loss of a M_r 78,000 marker in chemically induced transplantable carcinomas and primary carcinoma of human pancreas. *Cancer Res.* **48,** 2265–2272
11. Kato, T., Satoh, S., Okabe, H., Kitahara, O., Ono, K., Kihara, C., Tanaka, T., Tsunoda, T., Yamaoka, Y., Nakamura, Y., and Furukawa, Y. (2001) Isolation of a novel human gene, *MARKL1*, homologous to *MARK3* and its involvement in hepatocellular carcinogenesis. *Neoplasia* **3,** 4–9
12. Parsons, D. W., Wang, T. L., Samuels, Y., Bardelli, A., Cummins, J. M., DeLong, L., Silliman, N., Ptak, J., Szabo, S., Willson, J. K., Markowitz, S., Kinzler, K. W., Vogelstein, B., Lengauer, C., and Velculescu, V. E. (2005) Colorectal cancer: mutations in a signaling pathway. *Nature* **436,** 792
13. Zhang, B. B., Zhou, G., and Li, C. (2009) AMPK: an emerging drug target for diabetes and the metabolic syndrome. *Cell Metab.* **9,** 407–416
14. Hardie, D. G. (2008) AMPK: a key regulator of energy balance in the single cell and the whole organism. *Int. J. Obes.* **32,** S7–S12
15. Kahn, B. B., Alquier, T., Carling, D., and Hardie, D. G. (2005) AMP-activated protein kinase: ancient energy gauge provides clues to modern understanding of metabolism. *Cell Metab.* **1,** 15–25
16. Fu, A., Ng, A. C., Depatie, C., Wijesekara, N., He, Y., Wang, G. S., Bardeesy, N., Scott, F. W., Touyz, R. M., Wheeler, M. B., and Screaton, R. A. (2009) Loss of Lkb1 in adult β-cells increases β-cell mass and enhances glucose tolerance in mice. *Cell Metab.* **10,** 285–295
17. Granot, Z., Swisa, A., Magenheim, J., Stolovich-Rain, M., Fujimoto, W., Manduchi, E., Miki, T., Lennerz, J. K., Stoeckert, C. J., Jr., Meyuhas, O., Seino, S., Permutt, M. A., Piwnica-Worms, H., Bardeesy, N., and Dor, Y. (2009) LKB1 regulates pancreatic β-cell size, polarity, and function. *Cell Metab.* **10,** 296–308
18. Ikeda, Y., Sato, K., Pimentel, D. R., Sam, F., Shaw, R. J., Dyck, J. R., and Walsh, K. (2009) Cardiac-specific deletion of LKB1 leads to hypertrophy and dysfunction. *J. Biol. Chem.* **284,** 35839–35849
19. Jansen, M., Ten Klooster, J. P., Offerhaus, G. J., and Clevers, H. (2009) LKB1 and AMPK family signaling: the intimate link between cell polarity and energy metabolism. *Physiol. Rev.* **89,** 777–798
20. Jessen, N., Koh, H. J., Folmes, C. D., Wagg, C., Fujii, N., Løfgren, B., Wolf, C. M., Berul, C. I., Hirshman, M. F., Lopaschuk, G. D., and Goodyear, L. J. (2010) Ablation of LKB1 in the heart leads to energy deprivation and impaired cardiac function. *Biochim. Biophys. Acta* **1802,** 593–600
21. Koh, H. J., Arnolds, D. E., Fujii, N., Tran, T. T., Rogers, M. J., Jessen, N., Li, Y., Liew, C. W., Ho, R. C., Hirshman, M. F., Kulkarni, R. N., Kahn, C. R., and Goodyear, L. J. (2006) Skeletal muscle-selective knock-out of LKB1 increases insulin sensitivity, improves glucose homeostasis, and decreases TRB3. *Mol. Cell. Biol.* **26,** 8217–8227
22. Ohashi, K., Ouchi, N., Higuchi, A., Shaw, R. J., and Walsh, K. (2010) LKB1 deficiency in Tie2-Cre-expressing cells impairs ischemia-induced angiogenesis. *J. Biol. Chem.* **285,** 22291–22298
23. Sun, G., Tarasov, A. I., McGinty, J. A., French, P. M., McDonald, A., Leclerc, I., and Rutter, G. A. (2010) LKB1 deletion with the *RIP2.Cre* transgene modifies pancreatic β-cell morphology and enhances insulin secretion *in vivo*. *Am. J. Physiol. Endocrinol. Metab.* **298,** E1261–E1273
24. Thomson, D. M., Hancock, C. R., Evanson, B. G., Kenney, S. G., Malan, B. B., Mongillo, A. D., Brown, J. D., Hepworth, S., Fillmore, N., Parcell, A. C., Kooyman, D. L., and Winder, W. W. (2010) Skeletal muscle dysfunction in muscle-specific LKB1 knock-out mice. *J. Appl. Physiol.* **108,** 1775–1785
25. Lennerz, J. K., Hurov, J. B., White, L. S., Lewandowski, K. T., Prior, J. L., Planer, G. J., Gereau, R. W., 4th, Piwnica-Worms, D., Schmidt, R. E., and Piwnica-Worms, H. (2010) Loss of Par-1a/MARK3/C-TAK1 kinase leads to reduced adiposity, resistance to hepatic steatosis, and defective gluconeogenesis. *Mol. Cell. Biol.* **30,** 5043–5056
26. Drewes, G., Trinczek, B., Illenberger, S., Biernat, J., Schmitt-Ulms, G., Meyer, H. E., Mandelkow, E. M., and Mandelkow, E. (1995) Microtubule-associated protein/microtubule affinity-regulating kinase ($p110^{mark}$). A novel protein kinase that regulates tau-microtubule interactions and dynamic instability by phosphorylation at the Alzheimer-specific site serine 262. *J. Biol. Chem.* **270,** 7679–7688
27. Matenia, D., and Mandelkow, E. M. (2009) The tau of MARK: a polarized view of the cytoskeleton. *Trends Biochem. Sci* **34,** 332–342
28. Seshadri, S., Fitzpatrick, A. L., Ikram, M. A., DeStefano, A. L., Gudnason, V., Boada, M., Bis, J. C., Smith, A. V., Carassquillo, M. M., Lambert, J. C., Harold, D., Schrijvers, E. M., Ramirez-Lorca, R., Debette, S., Longstreth, W. T., Jr., Janssens, A. C., Pankratz, V. S., Dartigues, J. F., Hollingworth, P., Aspelund, T., Hernandez, I., Beiser, A., Kuller, L. H., Koudstaal, P. J., Dickson, D. W., Tzourio, C., Abraham, R., Antunez, C., Du, Y., Rotter, J. I., Aulchenko, Y. S., Harris, T. B., Petersen, R. C., Berr, C., Owen, M. J., Lopez-Arrieta, J., Varadarajan, B. N., Becker, J. T., Rivadeneira, F., Nalls, M. A., Graff-Radford, N. R., Campion, D., Auerbach, S., Rice, K., Hofman, A., Jonsson, P. V., Schmidt, H., Lathrop, M., Mosley, T. H., Au, R., Psaty, B. M., Uitterlinden, A. G., Farrer, L. A., Lumley, T., Ruiz, A., Williams, J., Amouyel, P., Younkin, S. G., Wolf, P. A., Launer, L. J., Lopez, O. L., van Duijn, C. M., and Breteler, M. M. (2010) Genome-wide analysis of genetic loci associated with Alzheimer disease. *JAMA* **303,** 1832–1840
29. Seidell, J. C., Muller, D. C., Sorkin, J. D., and Andres, R. (1992) Fasting respiratory exchange ratio and resting metabolic rate as predictors of weight gain: the Baltimore Longitudinal Study on Aging. *Int. J. Obes. Relat. Metab. Disord.* **16,** 667–674
30. Gosmanov, A. R., Umpierrez, G. E., Karabell, A. H., Cuervo, R., and Thomason, D. B. (2004) Impaired expression and insulin-stimulated phosphorylation of Akt-2 in muscle of obese patients with atypical diabetes. *Am. J. Physiol. Endocrinol. Metab.* **287,** E8–E15
31. Karlsson, H. K., Zierath, J. R., Kane, S., Krook, A., Lienhard, G. E., and Wallberg-Henriksson, H. (2005) Insulin-stimulated phosphorylation of the Akt substrate AS160 is impaired in skeletal muscle of type 2 diabetic subjects. *Diabetes* **54,** 1692–1697
32. Tsang, A., Hausenloy, D. J., Mocanu, M. M., Carr, R. D., and Yellon, D. M. (2005) Preconditioning the diabetic heart: the importance of Akt phosphorylation. *Diabetes* **54,** 2360–2364
33. Kobayashi, T., Taguchi, K., Yasuhiro, T., Matsumoto, T., and Kamata, K. (2004) Impairment of PI3K/Akt pathway underlies attenuated endothelial function in aorta of type 2 diabetic mouse model. *Hypertension* **44,** 956–962
34. Long, Y. C., and Zierath, J. R. (2006) AMP-activated protein kinase signaling in metabolic regulation. *J. Clin. Invest.* **116,** 1776–1783
35. Lizcano, J. M., Göransson, O., Toth, R., Deak, M., Morrice, N. A., Boudeau, J., Hawley, S. A., Udd, L., Mäkelä, T. P., Hardie, D. G., and Alessi, D. R. (2004) LKB1 is a master kinase that activates 13 kinases of the AMPK subfamily, including MARK/PAR-1. *EMBO J.* **23,** 833–843
36. Zhou, G., Myers, R., Li, Y., Chen, Y., Shen, X., Fenyk-Melody, J., Wu, M., Ventre, J., Doebber, T., Fujii, N., Musi, N., Hirshman, M. F., Goodyear, L. J., and Moller, D. E. (2001) Role of AMP-activated protein kinase in mechanism of metformin action. *J. Clin. Invest.* **108,** 1167–1174
37. Hardie, D. G. (2007) AMPK and SNF1: snuffing out stress. *Cell Metab.* **6,** 339–340
38. Li, Y., Xu, S., Mihaylova, M. M., Zheng, B., Hou, X., Jiang, B., Park, O., Luo, Z., Lefai, E., Shyy, J. Y., Gao, B., Wierzbicki, M., Verbeuren, T. J., Shaw, R. J., Cohen, R. A., and Zang, M. (2011) AMPK phosphorylates and inhibits

SREBP activity to attenuate hepatic steatosis and atherosclerosis in diet-induced insulin-resistant mice. *Cell Metab.* **13,** 376–388

39. Chen, M. B., McAinch, A. J., Macaulay, S. L., Castelli, L. A., O'Brien P, E., Dixon, J. B., Cameron-Smith, D., Kemp, B. E., and Steinberg, G. R. (2005) Impaired activation of AMP kinase and fatty acid oxidation by globular adiponectin in cultured human skeletal muscle of obese type 2 diabetics. *J. Clin. Endocrinol. Metab.* **90,** 3665–3672
40. Højlund, K., Mustard, K. J., Staehr, P., Hardie, D. G., Beck-Nielsen, H., Richter, E. A., and Wojtaszewski, J. F. (2004) AMPK activity and isoform protein expression are similar in muscle of obese subjects with and without type 2 diabetes. *Am. J. Physiol. Endocrinol. Metab.* **286,** E239–E244